Heliyon 10 (2024) e24568

Contents lists available at ScienceDirect

Heliyon

journal homepage: www.cell.com/heliyon

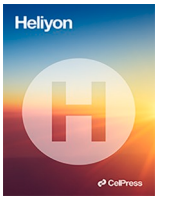

Research article

Apelin ameliorates sepsis-induced myocardial dysfunction via inhibition of NLRP3-mediated pyroptosis of cardiomyocytes

Zhi Cao [a,1], Weifeng Li [a,1], Zhuang Shao [a,1], Xinqiang Liu [a], Yi Zeng [a], Peijun Lin [a], Chuangqiang Lin [b], Yuechu Zhao [a], Ting Li [c], Zichao Zhao [a], Xin Li [a,b,c,**], Yuelin Zhang [a,c,***], Bei Hu [a,b,c,*]

[a] *Department of Emergency Medicine, Guangdong Provincial People's Hospital (Guangdong Academy of Medical Sciences), Southern Medical University, Guangzhou, Guangdong, China*
[b] *Medical College, Shantou University, Shantou, Guangdong, China*
[c] *School of Medicine, South China University of Technology, Guangzhou, China*

ARTICLE INFO

Keywords:
Myocardial dysfunction
Apelin
NLRP3 inflammasome
Pyroptosis

ABSTRACT

Sepsis-induced myocardial dysfunction (SMD) is the major cause of death in sepsis. Nucleotide-binding oligomerization domain-like receptor family pyrin domain containing 3 (NLRP3)-mediated pyroptosis contributes to the occurrence and development of SMD. Although Apelin confers direct protection against SMD, the potential mechanisms remain unclear. This study aimed to determine whether Apelin protects against SMD via regulation of NLRP3-mediated pyroptosis of cardiomyocytes. Experimental SMD was induced in wild-type (WT) control mice and Apelin knockout ($Apelin^{-/-}$) mice by cecal ligation and puncture (CLP). Neonatal mouse cardiomyocytes (NMCs) were treated with lipopolysaccharide (LPS) to simulate the physiological environment of SMD *in vitro*. The expression of Apelin was greatly decreased in the plasma from septic patients and septic mouse heart. Knockout of Apelin aggravated SMD, evidenced by decreased cardiac function, and increased cardiac fibrosis and NLRP3 inflammasome and pyroptosis levels in CLP-treated $Apelin^{-/-}$ mice compared with WT mice. Overexpression of Apelin activated the AMPK pathway and thereby inhibited NLRP3 inflammasome–mediated pyroptosis of NMCs induced by LPS *in vitro* These protective effects were partially abrogated by AMPK inhibitor. In conclusion, Apelin attenuated SMD by inhibiting NLRP3-mediated pyroptosis via activation of the AMPK pathway. Apelin may serve as a promising therapeutic target for SMD.

* Corresponding author. Department of Emergency Medicine, Guangdong Provincial People's Hospital, Guangdong Academy of Medical Sciences, Guangzhou, Guangdong, 510080, China.
** Corresponding author. Department of Emergency Medicine, Guangdong Provincial People's Hospital, Guangdong Academy of Medical Sciences, Guangzhou, Guangdong, 510080, China.
*** Corresponding author. Department of Emergency Medicine, Guangdong Provincial People's Hospital, Guangdong Academy of Medical Sciences, Guangzhou, Guangdong, 510080, China.
E-mail addresses: xlidoct@qq.com (X. Li), zhangyuelin1999@163.com (Y. Zhang), qhubei@hotmail.com (B. Hu).
[1] Zhi Cao, Weifeng Li, Zhuang Shao contributed equally to this work.

https://doi.org/10.1016/j.heliyon.2024.e24568
Received 4 September 2023; Received in revised form 17 December 2023; Accepted 10 January 2024
Available online 23 January 2024

1. Introduction

Sepsis, a complex life-threatening condition caused by infection, is the leading cause of morbidity and mortality encountered in emergency medicine [1,2]. It can lead to multiple organ damage with the heart the most important and frequently affected [3,4]. The incidence of sepsis-induced myocardial dysfunction (SMD) is reported to vary from 10 to 70 % in subjects with sepsis with mortality as high as 70–90 % [5,6]. Therefore, SMD has been the focus of much clinical and basic research over the past decades. Although a variety of mediators and signaling pathways, including mitochondrial dysfunction, abnormal metabolic reprogramming and overproduction of reactive oxygen species (ROS) have been found to be involved in SMD, their precise molecular mechanisms are not fully understood [7,8]. Understanding the mechanisms that underlie SMD will help in the exploration of therapeutic strategies for SMD.

Pyroptosis is a novel pro-inflammatory form of programmed cell death that is activated by nucleotide-binding oligomerization domain-like receptor family pyrin domain containing 3 (NLRP3) inflammasome. NLRP3 inflammasome activation promotes the precursor cleavage of Caspase-1 that initiates pyroptosis and production of the mature pro-inflammatory cytokines interleukin IL-1β and IL-18 [9,10]. Several studies have shown that NLRP3-mediated pyroptosis plays a critical role in regulating the pathogenesis of multiple cardiovascular diseases including myocardial infarction, myocarditis and diabetic cardiomyopathy [11–14]. There is also mounting evidence that NLRP3-mediated pyroptosis participates in the occurrence and development of SMD. It has been reported that Syringaresinol ameliorated SMD by inhibiting inflammation and NLRP3-mediated pyroptosis in mice [15]. More importantly, the NLRP3 inhibitor MCC950 improved heart function in SMD mice by reducing inflammatory factors and pyroptosis of cardiomyocytes via inhibition of the NLRP3/Caspase-1/IL-1β pathway [16]. Nonetheless the potential mechanism of NLRP3-mediated pyroptosis of cardiomyocytes in SMD remains unclear.

Apelin, an endogenous ligand for the APJ receptor, exerts essential roles in regulating cardiovascular physiology and pathophysiology [17,18]. Several isotypes of Apelin have been identified with differing number of amino acids, namely Apelin-13, -16, −17, −19, and −36 [19]. Apelin-13 has been intensively investigated and proven to play a critical role in cardiovascular disease and is cardioprotective [20,21]. Apelin treatment attenuated cardiac dysfunction caused by ischemia/reperfusion injury via inhibition of oxidative stress and cardiomyocyte apoptosis via regulation of ERK1/2 and the Akt signaling pathway [22]. Notably, Apelin also plays an essential role in protecting against SMD. Exogenous administration of Apelin has been shown to ameliorate lipopolysaccharide (LPS)-induced myocardial dysfunction *in vitro* by inhibiting inflammation and apoptosis and increasing autophagy via mediation of the TLR4/ERK1/2/NF-κB pathway [23]. Nonetheless it has not been determined whether Apelin protects against SMD by regulating NLRP3-mediated pyroptosis. This study aimed to investigate the potential role of Apelin-13 (abbreviated as Apelin in the text) in mediating the process of NLRP3-mediated pyroptosis via regulation of the AMPK pathway with consequent attenuation of SMD in mice. The results may provide a therapeutic strategy to reduce NLRP3-mediated pyroptosis in SMD.

Table 1
Matched patient characteristics.

Characteristics	Control	NSMD (n = 20)	SMD (n = 20)	p-Value
Age	64.00 (56.25–68.00)	62.85 (55.49–70.21)	62.15 (55.76–68.54)	0.874
Man	13 (65)	14 (70)	13 (65)	1
Medical history				
Hypertension	7 (35)	6 (30)	8(40)	0.942
Diabetes mellitus	4 (20)	3 (15)	3(15)	1
CKD	4 (20)	1 (5)	3(15)	0.90
Sources of infection				
Pulmonary		12 (60)	10(50)	0.751
Digestive		5 (25)	4(20)	1
Other		3 (15)	6(30)	0.451
SOFA Score	0	5.40 (3.95–6.85)	9.25(6.86–11.64)	<0.001
Laboratory				
Systolic blood pressure (mmHg)	124.00 (117.00–149.5)	113.50 (102.00–148.50)	96.00 (81.00–139.00)	<0.05
Diastolic blood pressure (mmHg)	72.50 (68.50–78.50)	68.50 (60.00–81.50)	58.50(50.50–68.00)	<0.001
Fibrinogen (g/L)	3.12 (2.71–3.45)	3.44 (2.58–4.43)	6.50 (5.39–7.38)	<0.001
CRP (mg/L)	5.60 (3.93–6.50)	95.60 (55.45–160.43)	125.00 (64.48–180.13)	<0.001
PCT (ng/mL)	0.01 (0.01–0.01)	5.58 (4.42–11.13)	50.76 (8.20–150.62)	<0.001
IL-6 (pg/mL)	4.25 (3.80–5.00)	41.20 (22.50–366.55)	228.50 (67.95-1272.50)	<0.001
BNP (pg/mL)	84.50 (58.00–97.25)	201.50 (129.00–437.70)	16634.65 (10979.91-22289.39)	<0.001
TNT (pg/mL)	8.60 (7.75–9.35)	22.30 (14.20–46.25)	640.97 (100.72–1382.65)	<0.001
CK-MB (U/L)	14.45 (12.88-17.30)	22.40 (11.08–33.72)	190.75 (44.30–425.79)	<0.001
CK (U/L)	72.50 (58.00–103.00)	127.50 (61.50–231.50)	662.50 (160.50–9274.50)	<0.001
Glucose (mmol/L)	6.40 (5.85–7.65)	7.25 (6.40–9.60)	8.95 (6.15–15.50)	<0.01
Lactic acid (mmol/L)	1.00 (0.80–1.25)	1.70 (1.25–3.55)	4.00 (2.60–7.70)	<0.001
LDH (U/L)	6739.00 (5684.50–7463.00)	6296.00 (5480.00–6867.50)	4288.50 (3464.50–6539.50)	<0.01
Transthoracic echocardiography				
Heart Rate	75 (69–86)	80 (75–92)	102 (92–111)	<0.001
E/A	1.70 (1.42–1.85)	1.57 (1.43–1.71)	0.95 (0.75–1.84)	<0.001
LVEF (%)	65.50 (64.25–67.0)	64.45 (62.98–65.92)	47.30 (43.81–50.79)	<0.001

CKD, Chronic kidney disease; CRP, *C*-reactive protein; PCT, procalcitonin; BNP, Brain Natriuretic Peptide; TNT, troponin T; CK-MB, Creatine Kinase-MB; E/A, early peak/atrial peak ratio; LVEF, Left Ventricular Ejection Fraction; IL-6, Interleukin- 6; CK, Creatine Kinase; LDH, Lactate dehydrogenase.

2. Methods and materials

2.1. Collection and storage of human plasma

Venous blood was collected from patients diagnosed with sepsis or septic shock, defined according to the Third International Consensus Definitions for Sepsis and Septic Shock (Sepsis-3). Patients with a history of previous cardiovascular disease were excluded from study. SMD was diagnosed by cTnT, CK, CK-MB, BNP level and cardiac ultrasound. Patients with sepsis or septic shock but no heart injury were classified as non-SMD (NSMD). Patients with no inflammatory response or cardiac dysfunction served as the control group. Written informed consent was obtained from all donors or a family member. The procedure was approved by the research ethics board of Guangdong Provincial People's Hospital (NO. KY-Z-2020-363-02). The demographic information of study subjects is summarized in Table 1. Blood samples of patients were centrifuged to obtain plasma that was frozen at −80 °C. Plasma level of Apelin was detected using an ELISA kit (MEIMIAN, China).

2.2. Cell culture

Neonatal mouse myocardial cells (NMC) were isolated and cultured as previously described [24]. Briefly, after washing with alcohol, mice were dissected and the hearts isolated and chopped with precooled phosphate buffered saline (PBS). Heart tissue was then mixed with 10 mg/ml collagenase and 30 mg/ml trypsin diluted in PBS and centrifuged at 1500 rpm for 5 min. Subsequently, cells were carefully suspended with 10 % fetal bovine serum (10099141, Gibco, USA) in DMEM/F12 (11330032, Gibco, USA) at 37 °C for 1 h. Finally, the supernatant was harvested and NMCs at P1 were plated in 24-well plates with collagen-coated glass coverslips at a density of 2×10^5 cells/well in an environment of 95 % O_2 and 5 % CO_2. Culture medium was changed daily. NMCs were treated with 1 μg/ml lipopolysaccharide (LPS, L4391, Sigma, USA) for 12h, 24h or 36h to induce a model of SMD in *vitro* [25]. To investigate the role of NLRP3-mediated pyroptosis, NMCs were pretreated with MCC950 (10 μM) for 30 min and then incubated with LPS for 24h.

2.3. Viral vector construction and infection

The lentivirus-carrying Apelin was generated and obtained from XindaiBio (Guangzhou, China). For stable transduction, NMCs at a confluence of 70–80 % were infected by lentivirus at a multiplicity of infection of 10 with polybrene (8 μg/mL) for 4 h and then cultured with complete medium for 48 h. Infection efficiency was determined by Western blotting. To determine whether Apelin protected against NLRP3 inflammasome-mediated pyroptosis in SMD via activation of the AMPK signaling pathway, NMCs overexpressing Apelin were pretreated with Compound C (20 μM) for 30 min and then incubated with LPS for 24h.

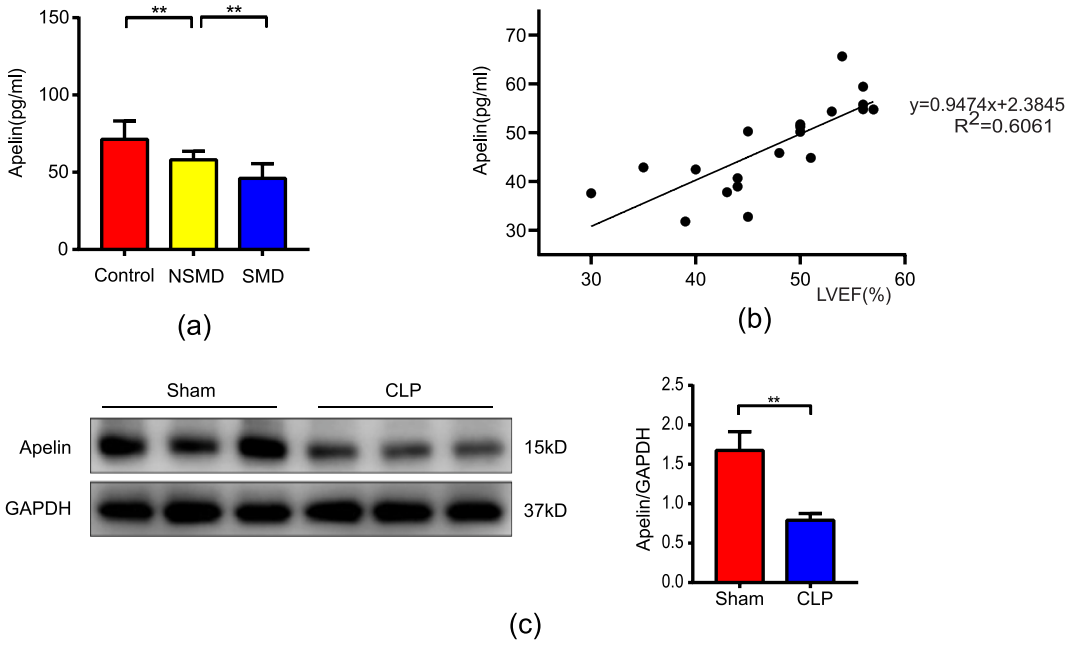

Fig. 1. Decreased Level of Apelin in SMD patients and Mouse Hearts. (a) Level of plasma Apelin in the plasma of control donors and patients with SMD and NSMD. (b) Relationship between the level of Apelin in the plasma and left ventricular ejection fraction (LVEF) in SMD patients. (c) Level of Apelin in heart tissue of sham and CLP-treated mice. Data are expressed as the mean ± SD of at least three independent experiments. *$p < 0.05$, **$p < 0.01$.

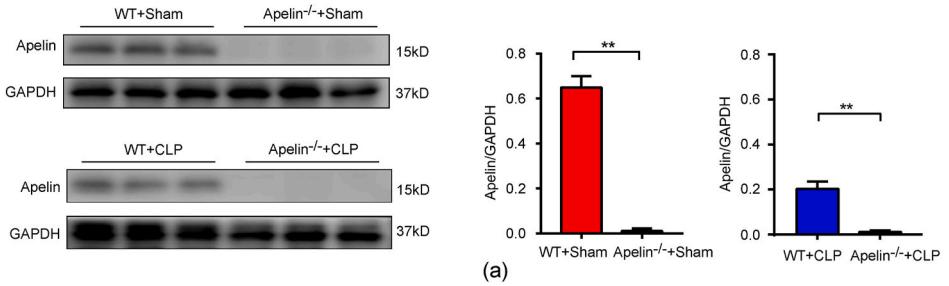

(a)

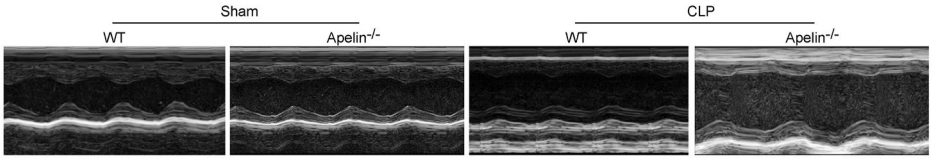

(b)

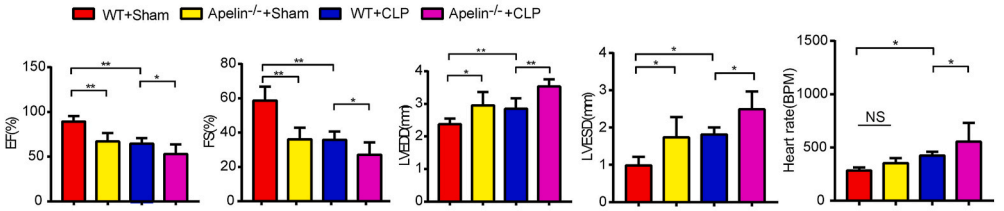

(c)

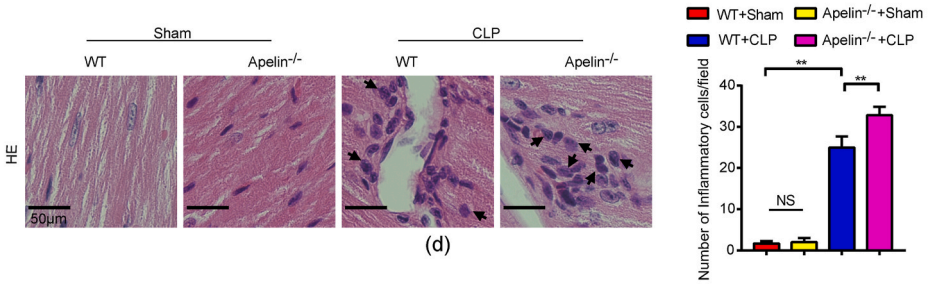

(d)

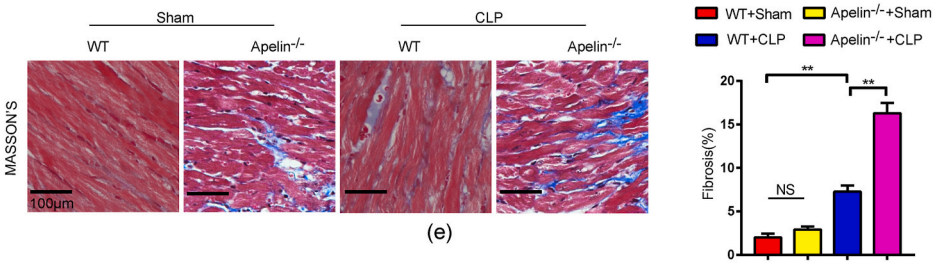

(e)

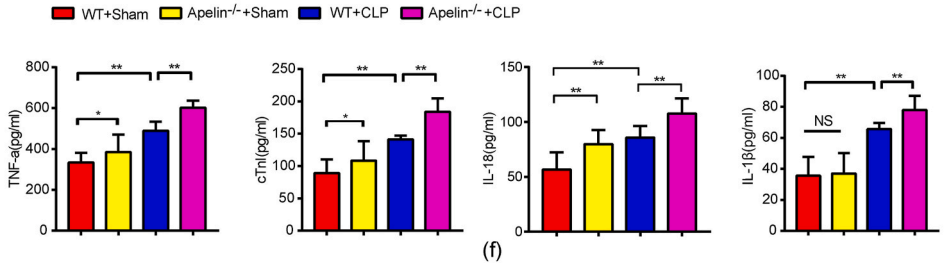

(f)

(caption on next page)

Fig. 2. Cardiomyocyte-specific Apelin deletion aggravated heart dysfunction in SMD mice. (a) Level of Apelin in heart tissue from WT Apelin$^{-/-}$ mice and CLP-treated WT and Apelin$^{-/-}$ mice. (b) Echocardiographic images captured at baseline or 24 h following CLP surgery in mice among the different groups. (c) Quantitative analysis of LVEF, LVFS, LVESD, LVEDD and heart rate at baseline or 24 h following CLP surgery in mice among the different groups. (d) HE staining and quantitative analysis of the number of inflammatory cells at baseline or 24 h following CLP surgery in mice among the different groups. Black arrows represent the nucleus of inflammatory cells. (e) Masson's trichrome staining and quantitative measurement of heart fibrosis at baseline or 24 h following CLP surgery in mice among the different groups. (f) Plasma level of cTnI, TNF-α, IL-18 and IL-1β at baseline or 24 h following CLP surgery in mice among the different groups. Data are expressed as the mean ± SD of at least three independent experiments. *$p < 0.05$, **$p < 0.01$.

2.4. TUNEL staining

Pyroptosis of NMCs among the different groups was evaluated by TUNEL staining according to the manufacturer's instructions (Roche, Switzerland). Briefly, NMCs were seeded into 24-well plates with cover slides and cultured to 70–80 % confluence, then stained with the kit and DAPI after fixing with ice-cold methanol. After washing with PBS three times, slides were photographed using a fluorescence microscope. Pyroptosis rate was calculated as the ratio of cells with green fluorescence to the total number of cells × 100 %.

2.5. ELISA

Blood samples from patients or mice were collected into an ethylene diamine Tet-Ra acetic acid (EDTA) tube and centrifuged at 3000 R/min for 15 min. Supernatant was collected and stored at −80 °C in a freezer. The concentration of IL-1β, IL-18, cTnI and TNF-α was measured using Enzyme linked Immunosorbent assay (ELISA) Kits (MEIMIAN, China) according to the kit instructions.

2.6. Immunofluorescence staining

Frozen sections of the heart were infiltrated with 0.1 % Triton X-100 and blocked with 10 % FBS. Next, slides were incubated with anti-cardiac Troponin T (1:100, bs-10648R, Bioss, USA), and anti-NLRP3 (1:100, AG-20B 0014, AdipoGen, USA) antibody overnight at 4 °C. After washing with PBS three times, the sections were incubated with fluorescent secondary antibodies (Abcam, Cambridge, UK) for 1 h at room temperature. Finally, the samples were incubated with DAPI and imaged under a microscope (Leica, Germany).

2.7. Western blotting

Heart tissue and NMCs from different groups were harvested. Total protein was extracted using a total protein extraction kit (Bestbio, Xi'an, China; BB-3101) and the concentration of each sample determined by BCA assay (231227, Thermo, USA). After adding loading buffer, the protein was denatured by placing in a water bath at 100 °C for 10 min, and 30ug protein subjected to sodium dodecyl sulfate polyacrylamide gel electrophoresis (SDS-PAGE). Next, the proteins were transferred onto PVDF membranes. After blocking with 5 % non-fat dry milk for 1h, membranes were incubated overnight at 4 °C with the following specific antibodies: anti-NLRP3 (1:1000, ab263899, abcam, UK), anti-ASC (1:1000, AG-25B-0006-C100, AdipoGen, USA), anti-Caspase-1 (1:1000, ab179515, abcam, UK), IL-1β (1:1000, 26048-1-AP, proteintech, USA), anti-IL-18 (1:1000, A1115, ABclonal, USA), anti-GSDMD (1:1000, ab209845, abcam, UK), anti-Apelin (1:1000, ab125213, Abcam, UK), anti-AMPK (1:1000, ab32047, abcam, UK), and anti-*p*-AMPK (1:1000, 2535s, CST, USA), GAPDH (1:10000, ab8245, abcam, UK). Subsequently, the membranes were washed with TBST three times and incubated with the secondary antibody (1:1000, CST, MA, USA) for at least 1 h at room temperature and exposed to radiography film in a dark room. Protein bands were analyzed by a ChemiDoc™ Touch Imaging System. Quantification of band intensity was performed using Image J software.

2.8. Mice

Wild type (WT) and Apelin$^{-/-}$ mice (C57BL/6J genetic background, 20–25 g, 8–10 weeks, male) were obtained from Gempharmatech Co., Ltd (China), and housed at the Laboratory Animal Center of Guangzhou Yongnuo under 12-h light-dark conditions. All animal experiments were approved by the Committee on the Use of Live Animals in Teaching and Research (CULTAR) of the Guangdong Provincial People's Hospital for Laboratory Animal Medicine (NO. KY-Z-2020-363-02).

2.9. CLP model

SMD was induced in WT and Apelin$^{-/-}$ mice by cecal ligation and puncture (CLP) as previously reported [26]. Mice were then randomly divided into four groups: Sham-WT (n = 6), Sham-Apelin$^{-/-}$ (n = 6), CLP-treated WT (n = 20) and CLP-treated Apelin$^{-/-}$ (n = 20). Mice were anesthetized by inhalation of 2 % isoflurane and fixed in a supine position. A longitudinal incision was made in the abdomen and the skin and abdominal muscles cut away, and the cecum carefully separated without vascular injury. Subsequently, the posterior 1/3 of the cecum was ligated with a non-absorbable suture, perforated twice using an 18-G needle and a small amount of intestinal content squeezed out. After operation, the cecum was replaced in the abdominal cavity and the abdominal muscle and skin closed successively after disinfection. Finally, mice were resuscitated by subcutaneous injection of normal saline. The CLP model was

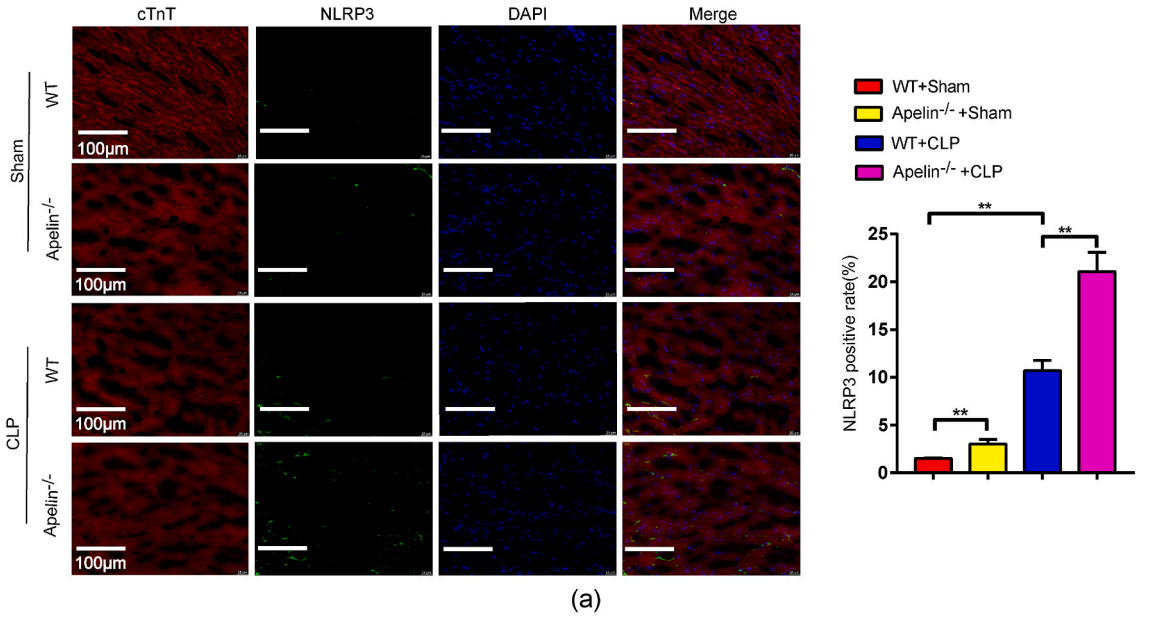

(caption on next page)

Fig. 3. Apelin inhibits NLRP3 inflammasome-mediated pyroptosis to protect against SMD. (a) NLRP3 inflammasome staining of heart tissue at baseline or 24 h following CLP surgery in mice among the different groups. (b) Western blotting and quantitative analysis of pyroptosis-related markers including NLRP3 inflammasome, ASC, activation of Caspase-1, GSDMD-NT, IL-1β and IL-18 in heart tissue of mice at baseline or 24 h following CLP surgery among the different groups. (c) TUNEL staining and quantitative analysis of TUNEL positive cells in heart tissue of mice at baseline or 24 h following CLP surgery among the different groups. Data are expressed as the mean ± SD of at least three independent experiments. *$p < 0.05$, **$p < 0.01$.

completed within 15 min. The sham operation mice underwent the same operation without cecum ligation and perforation.

2.10. Echocardiographic measurement

All mice were anesthetized by inhaled 2 % isoflurane. Heart function in each mouse was measured at 24 h following CLP surgery by transthoracic echocardiography (Ultramark 9; Soma Technology). Echocardiographic parameters including heart rate, left ventricular end-diastolic dimension (LVEDD, mm) and left ventricular end-systolic dimension (LVESD, mm) were calculated. Next, left ventricular ejection fraction (LVEF, %) and left ventricular fractional shortening (LVFS, %) were calculated.

2.11. HE staining

After echocardiography assessment, all mice were sacrificed by cervical dislocation under anaesthesia. Heart tissue was harvested, fixed, embedded, and cut into 5 μm slices. Next, heart sections from the four experimental groups were stained with hematoxylin eosin. Finally, changes to myocardial tissue structure were captured under a microscope.

2.12. Masson's staining

The heart sections from four experimental groups were subjected to Masson's trichrome staining according to the protocol (G1340, Solarbio, China). The ratio of fibrosis was calculated as the ratio of fibrotic area to total heart area × 100 %.

2.13. Statistical analysis

All results are expressed as mean ± SD. All experiments were performed at least three times *in vitro*. One-way analysis of variance (ANOVA) followed by the Bonferroni test was used for statistical comparison among multiple groups, and comparison between two groups made using unpaired Student T test. Data were analyzed by Graphpad Prism 7.0 software and $P < 0.05$ considered statistically significant.

3. Results

3.1. Decreased level of Apelin in SMD patients and mouse hearts

To determine the possible role of Apelin in the pathogenesis of SMD, we initially examined the level of Apelin in the plasma of control donors (n = 20), and patients with SMD (n = 20) and NSMD (n = 20). The characteristics of Sepsis-induced myocardial dysfunction are shown in Table 1. Compared with controls and NMSD, the LVEF was greatly reduced in MSD patients (Table 1). The myocardial injury markers such CK, TNT and BNP was much higher in MSD patients than controls and NMSD (Table 1). In addition, we also analyzed the blood pressure of the controls, NMSD and MSD patients (Table 1). The systolic blood and diastolic blood were greatly decreased in MSD patients compared with controls and NMSD patients. The level of plasma Apelin from SMD patients was much lower than that in the control donors and NSMD patients (Fig. 1a). Importantly, the content of plasma Apelin was significantly and positively associated with LVEF in SMD patients (Fig. 1b). We also established an SMD model in wild-type (WT) mice using CLP. Similarly, there was a remarkable reduction in Apelin in the heart tissue of SMD mice compared with WT mice (Fig. 1c). Collectively, these findings suggested that reduction of Apelin was closely associated with the progression of both human and mouse SMD.

3.2. Cardiomyocyte-specific apelin deletion aggravated heart dysfunction in SMD mice

To further investigate the impact of Apelin on SMD, we established an SMD model in a cardiomyocyte-specific inducible Apelin knockout mouse (Apelin$^{-/-}$ mice). In the current study, 14 mice survived in the CLP-treated WT group and 11 in the CLP-treated Apelin$^{-/-}$ group. No mouse succumbed in the Sham-WT group or Sham-Apelin$^{-/-}$ group. Compared with WT mice, no expression of Apelin was detected in the heart tissue of Apelin$^{-/-}$ mice, indicating that Apelin$^{-/-}$ mice had been successfully generated (Fig. 2a). Subsequently, Apelin$^{-/-}$ and WT mice were subjected to CLP surgery to generate SMD. The representative echocardiographic images are shown in Fig. 2b. Compared with WT mice, Apelin$^{-/-}$ mice displayed decreased EF and FS at baseline, indicating heart dysfunction (Fig. 2c). After CLP surgery, both WT mice and Apelin$^{-/-}$ mice exhibited decreased EF and FS compared with baseline (Fig. 2c). Notably, both EF and FS were further decreased in Apelin$^{-/-}$ mice compared with WT mice (Fig. 2c). Importantly, after CLP surgery, LVEDD and LVESD was greatly increased in WT mice and Apelin$^{-/-}$ mice and further increased in Apelin$^{-/-}$ mice (Fig. 2c), suggesting

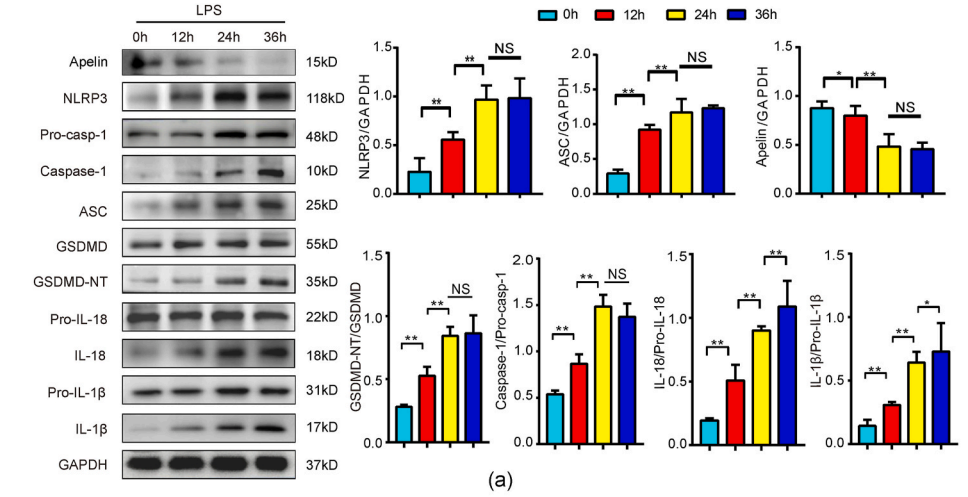

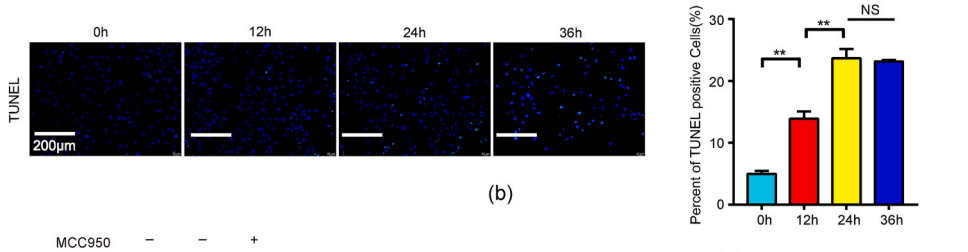

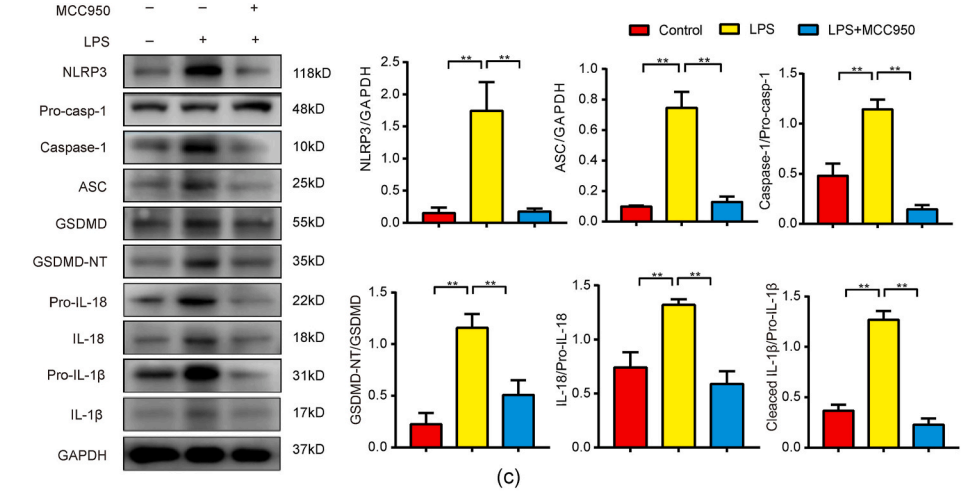

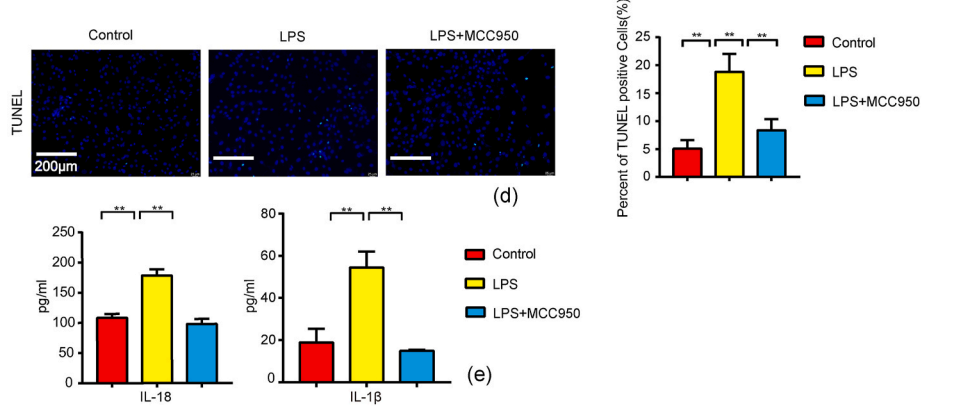

(caption on next page)

Fig. 4. Downregulation of Apelin is positively correlated with pyroptosis in LPS-induced SMD *in vitro*. (a) Western blotting and quantitative analysis of Apelin and pyroptosis-related markers in NMCs following LPS treatment for 0 h, 12 h, 24 h and 36 h. (b) TUNEL staining and quantitative analysis of TUNEL positive cells in NMCs with LPS treatment for 0 h, 12 h, 24 h and 36 h. (c) Western blotting and quantitative analysis of pyroptosis-related protein makers in NMCs, LPS treated NMCs and LPS + MCC950 treated NMCs. (d) TUNEL staining and quantitative analysis of TUNEL positive cells in NMCs, LPS-treated NMCs and LPS + MCC950 treated NMCs. (e) Level of inflammatory cytokines IL-18 and IL-1β in the supernatant from NMCs, LPS treated NMCs or LPS + MCC950 treated NMCs. Data are expressed as the mean ± SD of at least three independent experiments. *$p < 0.05$, **$p < 0.01$.

that Apelin deficiency aggravated heart dysfunction in the presence of sepsis. Moreover, heart rate was greatly increased in WT mice and Apelin$^{-/-}$ mice and further increased in Apelin$^{-/-}$ mice after CLP surgery (Fig. 2c). HE staining showed that CLP-treated WT mice exhibited apparent inflammatory infiltration of myocardial tissue and this phenomenon was worse in CLP-treated Apelin$^{-/-}$ mice (Fig. 2d). Masson's trichrome staining was performed to evaluate the influence of Apelin deletion on cardiac fibrosis induced by CLP in mice. As shown in Fig. 2e, after CLP surgery, cardiac fibrosis was significantly increased in WT mice compared with baseline (Fig. 2e). Importantly, CLP-treated Apelin$^{-/-}$ mice exhibited increased cardiac fibrosis compared with WT mice (Fig. 2e). In addition, plasma concentration of inflammatory cytokines (TNF-a、IL-18 and IL-1β) and a biochemical marker of cardiac damage (cTnI) was significantly increased in CLP-treated WT mice and these cytokines were further markedly elevated in CLP-treated Apelin$^{-/-}$ mice (Fig. 2f). Collectively, these results demonstrated that Apelin deficiency in cardiomyocytes aggravated heart dysfunction in SMD mice.

3.3. Apelin deletion aggravated heart dysfunction via activation of NLRP3 inflammasome-mediated pyroptosis

Next, we aimed to determine whether NLRP3 inflammasome-mediated pyroptosis was involved in SMD and whether Apelin deletion would aggravate heart dysfunction via activation of NLRP3 inflammasome-mediated pyroptosis. Immunofluorescence staining showed that the expression of NLRP3 inflammasome in heart tissue was greatly increased in WT mice and Apelin$^{-/-}$ mice following CLP treatment when compared with the control group (Fig. 3a). Importantly, deletion of Apelin further enhanced CLP-induced NLRP3 inflammasome in the heart tissue of mice (Fig. 3a). Next, we examined the effects of Apelin deficiency on CLP-induced pyroptosis in heart tissue. Compared with WT mice, expression of pyroptosis-related markers including NLRP3, ASC, the ratio of Caspase-1/pro-Caspase-1, GSDMD-NT/GSDMD as well as IL-1β/pro-IL-1β and IL-18/pro-IL-18 in was markedly increased in the heart tissue of CLP-treated Apelin$^{-/-}$ mice (Fig. 3b). The percentage of TUNEL-positive staining cells was also increased in the heart tissue of CLP-treated Apelin$^{-/-}$ mice compared with WT mice (Fig. 3c). These results demonstrated that deletion of Apelin activated NLRP3 inflammasome-mediated pyroptosis of cardiomyocytes in CLP-treated mice.

3.4. Downregulation of Apelin is positively correlated with pyroptosis in LPS-induced SMD in vitro

We then investigated the relationship between Apelin and NLRP3 inflammasome-mediated pyroptosis in LPS-induced SMD *in vitro*. Following LPS treatment, the protein level of Apelin was reduced in cardiomyocytes in a time dependent manner under LPS challenge with the reduction most obvious after treatment for 24 h (Fig. 4a). Similarly, the protein level of NLRP3, ASC, the ratio of Caspase-1/pro-Caspase-1, GSDMD-NT/GSDMD as well as IL-1β/pro-IL-1β and IL-18/pro-IL-18 was markedly increased in NMCs after LPS treatment for 24 h (Fig. 4a). The percentage of TUNEL staining cells was also increased in NMCs, indicating activated pyroptosis under LPS challenge (Fig. 4b). To further verify that LPS induced NLRP3 inflammasome-mediated pyroptosis in cardiomyocytes, we treated NMCs with NLRP3 inhibitor MCC950 under LPS challenge. Western blotting revealed that MCC950 treatment significantly downregulated the expression of NLRP3, ASC, the ratio of Caspase-1/pro-Caspase-1, GSDMD-NT/GSDMD as well as IL-1β/pro-IL-1β and IL-18/pro-IL-18 in NMCs induced by LPS (Fig. 4c). Similarly, MCC950 treatment partially inhibited pyroptosis of NMCs induced by LPS as evidenced by the reduced percentage of TUNEL staining cells (Fig. 4d). More importantly, ELISA results demonstrated that LPS treatment upregulated the expression of IL-18 and IL-1β in NMCs and these effects were partially abrogated by MCC950 (Fig. 4e). Collectively, these data suggested that Apelin is closely associated with NLRP3 inflammasome-mediated pyroptosis in LPS-induced SMD *in vitro*.

3.5. Overexpression of Apelin attenuates LPS-induced SMD in vitro

Given the downregulation of Apelin and upregulation of NLRP3 inflammasome-mediated pyroptosis in NMCs under LPS treatment, we investigated the effects of Apelin on LPS-induced pyroptosis in NMCs. We overexpressed Apelin in NMCs with adenovirus. As shown in Fig. 5a, the level of Apelin was greatly increased in NMCs following infection with adenovirus carrying Apelin (Fig. 5a). Overexpression of Apelin significantly decreased production of IL-18 and IL-1β in NMCs induced by LPS (Fig. 5b). Consistently, overexpression of Apelin significantly attenuated LPS-induced NLRP3 inflammasome-mediated pyroptosis as evidenced by a reduced protein level of NLRP3, ASC, ratio of Caspase-1/pro-Caspase-1, GSDMD-NT/GSDMD as well as IL-1β/pro-IL-1β and IL-18/pro-IL-18 (Fig. 5c). Overexpression of Apelin also decreased the percentage of TUNEL-positive cells in LPS-treated NMCs (Fig. 5d). These data showed that overexpression of Apelin ameliorated NLRP3 inflammasome-mediated pyroptosis in cardiomyocytes induced by LPS.

3.6. Apelin protected against NLRP3 inflammasome-mediated pyroptosis in SMD through activation of the AMPK signaling pathway

Accumulating evidence has shown that the AMPK signaling pathway plays a critical role in regulating NLRP3 inflammasome-

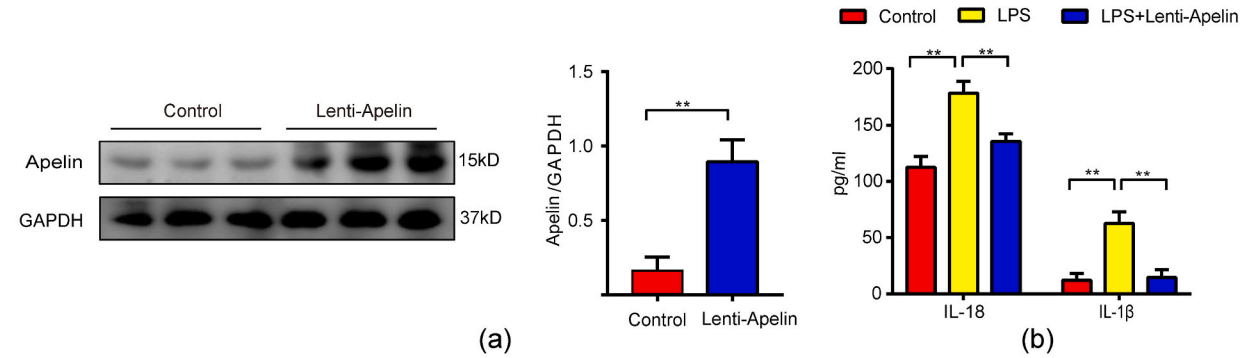

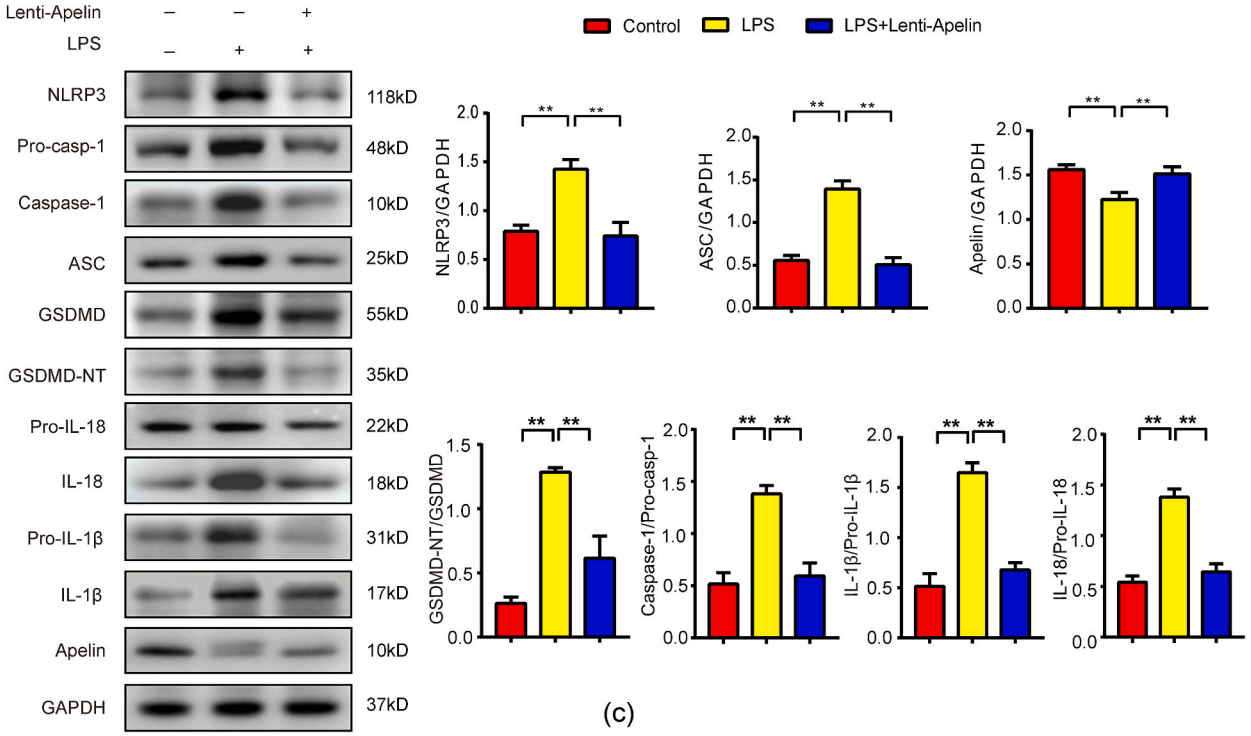

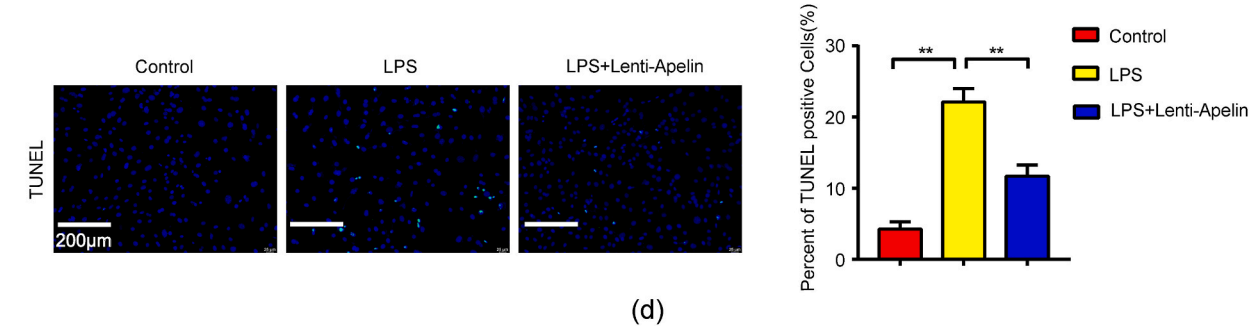

(caption on next page)

Fig. 5. Overexpression of Apelin alleviates LPS-induced SMD *in vitro*. (a) Western blotting and quantitative analysis of Apelin in NMCs after lentivirus infection. (b) Level of IL-18 and IL-1β in the supernatant from NMCs, LPS treated NMCs and LPS + Lenti-Apelin treated NMCs. (c) Western blotting and quantitative analysis of pyroptosis-related protein makers in NMCs, LPS treated NMCs and LPS + Lenti-Apelin treated NMCs. (d) TUNEL staining and quantitative analysis of TUNEL positive cells in NMCs, LPS treated NMCs and LPS + Lenti-Apelin treated NMCs. Data are expressed as the mean ± SD of at least three independent experiments. $^{*}p < 0.05$, $^{**}p < 0.01$.

mediated pyroptosis [27]. We therefore aimed to determine whether Apelin mediated NLRP3 inflammasome-mediated pyroptosis via regulation of that pathway. We first examined the expression of *p*-AMPK in SMD mice. Compared with WT mice, expression of *p*-AMPK was robustly decreased (Fig. 6a). Subsequently, Compound C, the inhibitor of the AMPK activation, was added to culture medium of Apelin-overexpressed NMCs under LPS stimulation. Compound C treatment greatly downregulated the expression of *p*-AMPK in Apelin-overexpressed NMCs under LPS stimulation (Fig. 6b). Importantly, Compound C treatment partially reversed the inhibition of NLRP3 inflammasome-mediated pyroptosis in Apelin-overexpressed NMCs under LPS stimulation as evidenced by increased levels of NLRP3, ASC, ratio of Caspase-1/pro-Caspase-1, GSDMD-NT/GSDMD as well as IL-1β/pro-IL-1β and IL-18/pro-IL-18 (Fig. 6c). Similarly, Compound C treatment increased the percentage of TUNEL-positive staining cells (Fig. 6d) and also elevated the expression of IL-18 and IL-1β (Fig. 6e). Collectively, these findings indicated that Apelin protected against NLRP3 inflammasome-mediated pyroptosis in SMD through activation of the AMPK signaling pathway.

4. Discussion

In this study, we present several major findings (Fig. 7). First, the content of Apelin was greatly decreased in septic patients and the septic mouse heart. Second, Apelin deficiency aggravated SMD in mice via activation of NLRP3 inflammasome-mediated pyroptosis in cardiomyocytes. Third, overexpression of Apelin attenuated LPS-induced cardiomyocyte injury via downregulation of NLRP3-mediated pyroptosis. Fourth, Apelin inhibited NLRP3-mediated pyroptosis to attenuate cardiomyocyte injury via activation of the AMPK signaling pathway. Thus, Apelin might serve as a promising therapeutic strategy for SMD treatment.

SMD is a severe disease with high mortality worldwide. Despite advances in pharmacological therapy including prophylactic antibiotics and intravenous immunoglobulin, there remains no effective treatment [6,28–30]. The main hurdle is a poor understanding of the molecular mechanisms that govern SMD. Although the potential mechanisms underlying SMD are unclear, it is well documented to be triggered by mitochondrial dysfunction, endoplasmic reticulum stress and dysregulated autophagy leading to heart injury [31–33]. Recently, NLRP3-mediated pyroptosis has been identified to be involved in SMD. It has been established that zinc finger antisense 1 aggravates the development of SMD via targeting of NLRP3-mediated pyroptosis of cardiomyocytes [34]. Knockout of a stimulator of interferon genes has been shown to alleviate heart injury in LPS-induced SMD mice via suppression of NLRP3-mediated pyroptosis of cardiomyocytes [25]. In contrast, another study showed that NLRP3 knockout mice exhibited worse cardiac dysfunction than WT control mice [35]. These data suggest that NLRP3 inflammasome exerts multifaceted effects in regulating heart homeostasis. In the current study, level of NLRP3, ASC and pyroptosis-related proteins including GSDMD-NT and Caspase-1 was greatly enhanced in the heart tissue of septic mice and LPS-treated NMCs. Moreover, the level of IL-18 and IL-1β was significantly increased. Furthermore, CLP operation also increased fibrosis and elevated the protein level of fibrotic markers in SMD mice [36]. Similarly, in the current study, cardiac fibrosis was also greatly increased in SMD mice. This is may have been due to NLRP3-mediated inflammation induced activation of cardiac fibroblasts. These results indicated that NLRP3-mediated pyroptosis plays a critical role in regulating SMD. Our study showed that NLRP3-mediated pyroptosis contributes to SMD development. Nonetheless because of the increased TUNEL positive cells in LPS-treated NMCs and CLP-treated mice, we could not exclude the possibility that apoptotic cardiomyocytes also regulate SMD. Given the multifaceted effects on heart function, direct inhibition of NLRP3 inflammasome may not be an optimal strategy for SMD treatment, so identification of the critical mediator that regulates NLRP3-mediated pyroptosis is vital for SMD treatment.

An increasing number of studies have demonstrated that Apelin plays an important role in the regulation of cardiovascular function including myocardial inflammation, contractility and vascular tension [37,38]. Apelin treatment has been shown to improve cardiac dysfunction and attenuate fibrosis in a rat model of myocardial infarction via downregulation of ROS level [39]. Apelin deficiency resulted in the progressive development of heart failure as evidenced by impaired cardiac contractility in pressure overload treated mice [40]. Apelin inhibited phenylephrine-induced cardiac hypertrophy by activating the PI3K/AKT/mTOR signaling pathway [41]. Given the findings that Apelin exerts cardioprotective effects, we speculated that Apelin may protect against myocardial injury in SMD, and if so, may be via regulation of NLRP3-mediated pyroptosis. It has been reported that Apelin administration antagonizes myocardial injury, manifested by lowered left ventricular end-diastolic pressure and elevated + LVdp/dt (max), by inhibiting inflammatory responses in mice with CLP-induced SMD [42]. In the current study, level of Apelin was greatly reduced in septic patients and the septic mouse heart, indicating that Apelin may be involved in regulating SMD. Importantly, our *in vivo* study showed that knockout of Apelin aggravated myocardial impairment in CLP-treated Apelin$^{-/-}$ mice via increasing NLRP3-mediated pyroptosis. It has been reported that Apelin-13 alleviated cardiac fibrosis in mice with myocardial infarction, indicating that Apelin-13 exerts an anti-fibrotic effect [43]. We also found that knockout of Apelin aggravated formation of cardiac fibrosis in CLP-treated Apelin$^{-/-}$ mice. In our *in vitro* study, we further verified that overexpression of Apelin functionally attenuated LPS-induced NMC injury via downregulation of NLRP3-mediated pyroptosis. Our results clearly suggest that Apelin may protect against SMD by inhibiting NLRP3-mediated pyroptosis in NMCs induced by LPS *in vitro* or CLP *in vivo*.

There are multiple lines of evidence that the AMPK signaling pathway participates in mediating NLRP3-mediated pyroptosis. Nicorandil has been shown to confer protection against coronary microembolization-induced myocardial injury by inhibiting NLRP3-

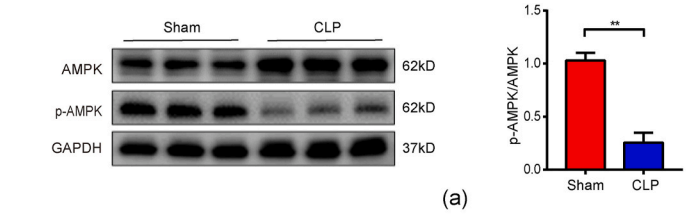

(a)

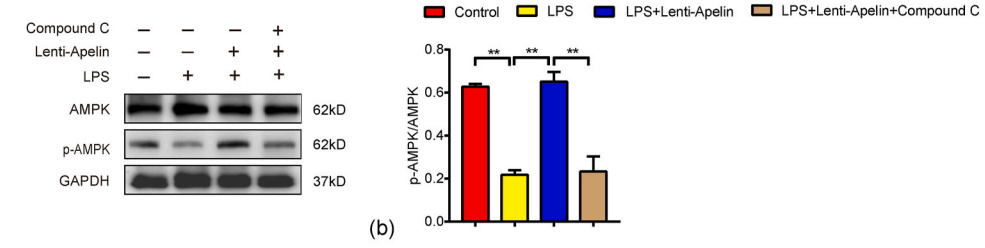

(b)

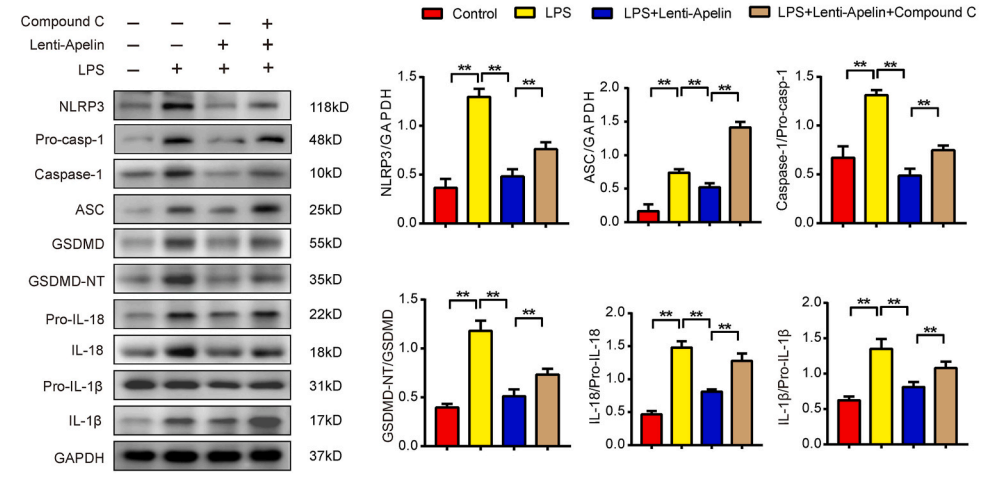

(c)

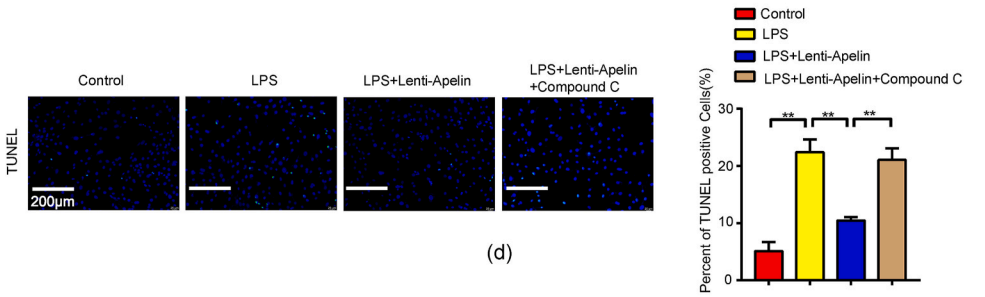

(d)

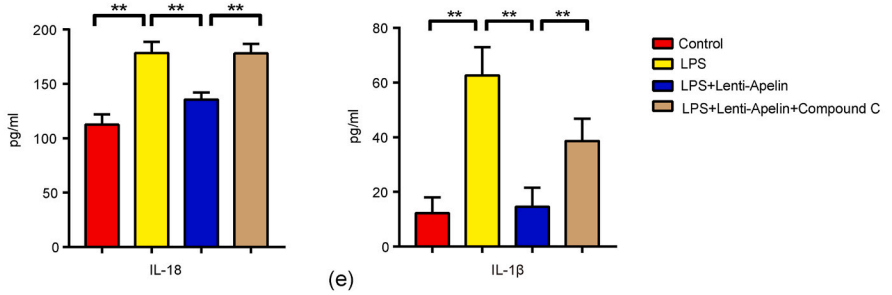

(e)

(caption on next page)

Fig. 6. Apelin protected against NLRP3 inflammasome-mediated pyroptosis in MD via the AMPK signaling pathway. (a) Western blotting and quantitative analysis of the expression of *p*-AMPK in heart tissue of WT and CLP treated mice. (b) Western blotting and quantitative analysis of *p*-AMPK phosphorylation in NMCs with or without LPS, LPS + Lenti-Apelin or LPS + Lenti-Apelin + Compound C treatment. (c) Western blotting and quantitative analysis of pyroptosis-related makers in NMCs with or without LPS, LPS + Lenti-Apelin or LPS + Lenti-Apelin + Compound C treatment. (d) TUNEL staining and quantitative analysis of TUNEL positive cells in NMCs with or without LPS, LPS + Lenti-Apelin or LPS + Lenti-Apelin + Compound C treatment. (e) Plasma level of IL-18 and IL-1β in cell supernatant from NMCs with or without LPS, LPS + Lenti-Apelin or LPS + Lenti-Apelin + Compound C treatment. Data are expressed as the mean ± SD of at least three independent experiments. $*p < 0.05$, $**p < 0.01$.

mediated pyroptosis of cardiomyocytes via regulation of the AMPK signaling pathway [44]. High glucose and ischemia/reperfusion-induced myocardial injury were ameliorated via mediation of cardiomyocyte pyroptosis by regulating the AMPK/NLRP3 signaling pathway [45]. Interestingly, Apelin exerts cardioprotective effects also via mediation of the AMPK pathway. Apelin administration has been reported to attenuate bupivacaine-induced cardiotoxicity via enhancement of mitochondrial energy metabolism by regulating AMPK [46]. In another study, Apelin-13 ameliorated ischemia-reperfusion-induced heart injury via downregulation of ER-dependent apoptotic pathways by activating PI3K/Akt, AMPK, and the ERK signaling pathway [47]. These results prompted us to determine whether Apelin protects against SMD by inhibition of NLRP3-mediated pyroptosis via regulation of the AMPK signaling pathway. Indeed, we found that overexpression of Apelin did attenuate LPS-induced pyroptosis of NMCs via activation of the AMPK signaling pathway, and this effect was partially abrogated by an AMPK inhibitor.

Although our study has several promising findings, several limitations should be acknowledged. First, There is mounting evidence that overproduction of ROS plays a critical role in the regulation of SMD [48,49]. Although we showed that NLRP3 mediated pyroptosis and inflammation contribute to SMD in the current study, whether Apelin attenuates SMD via regulation of ROS production warrants investigation. More importantly, further investigation is required to determine which of NLRP3-mediated pyroptosis or ROS production is more important to SMD development. Second, although overexpression of Apelin attenuated LPS-induced cardiomyocyte injury *in vitro*, whether Apelin administration can ameliorate SMD needs to be verified *in vivo*. Third, in addition to the AMPK pathway, it has not been determined whether Apelin inhibits NLRP3-mediated pyroptosis to attenuate SMD via other signaling pathways. Fourth, the NLR family has several members including NLRP1, NLRP3, NLRP6 and NLRP4. Whether other inflammasomes that may regulate SMD are affected requires further investigation.

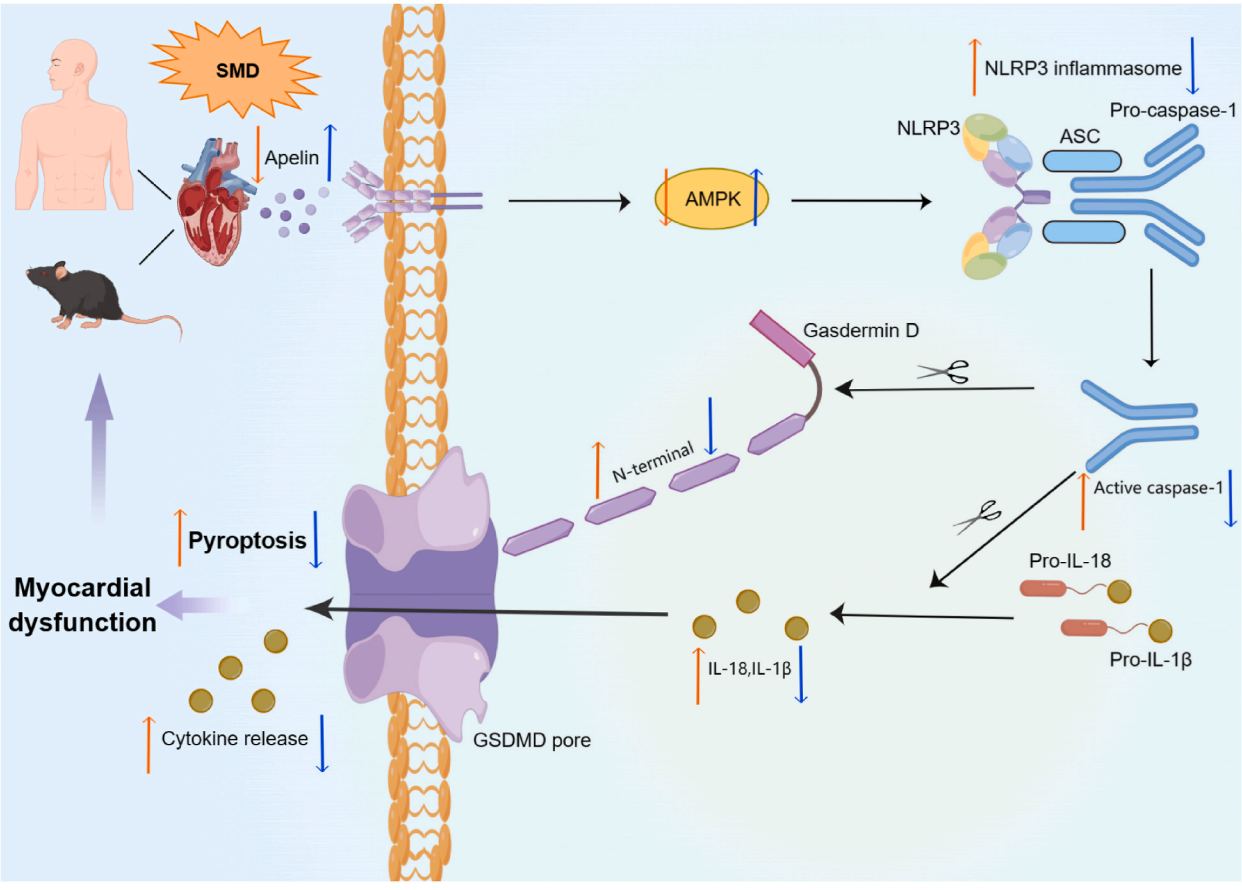

Fig. 7. The proposed mechanisms involved in Apelin-ameliorated sepsis-induced-myocardial dysfunction by inhibition of NLRP3-mediated pyroptosis.

5. Conclusion

Apelin protects against SMD by inhibiting NLRP3-mediated pyroptosis via activation of the AMPK pathway. Apelin deficiency downregulated the AMPK pathway and thereby aggravated NLRP3-mediated pyroptosis, leading to heart injury in septic mice. Our study highlights the therapeutic potential of Apelin in the treatment of sepsis-related cardiac remodeling and dysfunction.

Funding

This research was in part supported by the National Natural Science Grant of China (No. 82072139 to B.H.; No. 82072225 to X.L.), Natural Science Foundation for Distinguished Scholarship of Guangdong Province of China (2022B1515020104 to Y. Z.), the Fund for Distinguished Young Scholar of GDPH (No. KJ012021184 to B.H.; KY0120220132 to Y. Z.), the High-level Hospital Construction Project of Guangdong Provincial People's Hospital (No. KJ012019448 to B.H.), Science and Technology Program of Guangzhou (No. 202102080123) , the Science and Technology Planning Project of Guangzhou (202102080003 to Weifeng Li) and Scientific research project of Guangdong traditional Chinese Medicine Bureau (No. 20211009).

Data availability statement

The dataset supporting the conclusions of this article is included within this article and is available from the corresponding author upon request.

No public data was used for the research described in this article, so we didn't deposit any data associated with our research into a publicly available repository.

Ethical statement

This study was reviewed and approved by the Ethics Committee of Guangdong Provincial People's Hospital (No. KY-Z-2020-363-02). All participants/patients (or their proxies/legal guardians) provided informed consent to participate in the study.

CRediT authorship contribution statement

Zhi Cao: Writing – original draft, Software, Formal analysis. **Weifeng Li:** Methodology, Investigation. **Zhuang Shao:** Software, Project administration. **Xinqiang Liu:** Investigation. **Yi Zeng:** Data curation. **Peijun Lin:** Software. **Chuangqiang Lin:** Project administration, Data curation. **Yuechu Zhao:** Software. **Ting Li:** Software. **Zichao Zhao:** Investigation. **Xin Li:** Writing – review & editing, Data curation. **Yuelin Zhang:** Writing – review & editing, Formal analysis. **Bei Hu:** Writing – review & editing, Resources, Methodology.

Declaration of competing interest

The authors declare that they have no known competing financial interests or personal relationships that could have appeared to influence the work reported in this paper.

Acknowledgements

The authors thank Ms. Sarah M. Aglionby for editing the manuscript.

Appendix A. Supplementary data

Supplementary data to this article can be found online at https://doi.org/10.1016/j.heliyon.2024.e24568.

References

[1] J. Vandewalle, C. Libert, Sepsis: a failing starvation response, Trends Endocrinol. Metabol. 33 (4) (2022) 292–304, https://doi.org/10.1016/j.tem.2022.01.006.
[2] M. Cecconi, L. Evans, M. Levy, A. Rhodes, Sepsis and septic shock, Lancet 392 (10141) (2018) 75–87, https://doi.org/10.1016/s0140-6736(18)30696-2.
[3] L. Martin, M. Derwall, S. Al Zoubi, E. Zechendorf, D.A. Reuter, C. Thiemermann, et al., The septic heart: current understanding of molecular mechanisms and clinical Implications, Chest 155 (2) (2019) 427–437, https://doi.org/10.1016/j.chest.2018.08.1037.
[4] Y. Nong, X. Wei, D. Yu, Inflammatory mechanisms and intervention strategies for sepsis-induced myocardial dysfunction, Immun Inflamm Dis 11 (5) (2023) e860, https://doi.org/10.1002/iid3.860.
[5] S.M. Hollenberg, M. Singer, Pathophysiology of sepsis-induced cardiomyopathy, Nat. Rev. Cardiol. 18 (6) (2021) 424–434, https://doi.org/10.1038/s41569-020-00492-2.
[6] M.W. Merx, C. Weber, Sepsis and the heart, Circulation 116 (7) (2007) 793–802, https://doi.org/10.1161/circulationaha.106.678359.
[7] R. Wang, Y. Xu, Y. Fang, C. Wang, Y. Xue, F. Wang, et al., Pathogenetic mechanisms of septic cardiomyopathy, J. Cell. Physiol. 237 (1) (2022) 49–58, https://doi.org/10.1002/jcp.30527.

[8] S.J. Beesley, G. Weber, T. Sarge, S. Nikravan, C.K. Grissom, M.J. Lanspa, et al., Septic cardiomyopathy, Crit. Care Med. 46 (4) (2018) 625–634, https://doi.org/10.1097/ccm.0000000000002851.

[9] S.K. Hsu, C.Y. Li, I.L. Lin, W.J. Syue, Y.F. Chen, K.C. Cheng, et al., Inflammation-related pyroptosis, a novel programmed cell death pathway, and its crosstalk with immune therapy in cancer treatment, Theranostics 11 (18) (2021) 8813–8835, https://doi.org/10.7150/thno.62521.

[10] R.C. Coll, K. Schroder, P. Pelegrín, NLRP3 and pyroptosis blockers for treating inflammatory diseases, Trends Pharmacol. Sci. 43 (8) (2022) 653–668, https://doi.org/10.1016/j.tips.2022.04.003.

[11] K.Z. Zhang, X.Y. Shen, M. Wang, L. Wang, H.X. Sun, X.Z. Li, et al., Retinol-binding protein 4 promotes cardiac injury after myocardial infarction via inducing cardiomyocyte pyroptosis through an interaction with NLRP3, J. Am. Heart Assoc. 10 (22) (2021) e022011, https://doi.org/10.1161/jaha.121.022011.

[12] Q. Wang, J. Wu, Y. Zeng, K. Chen, C. Wang, S. Yang, et al., Pyroptosis: a pro-inflammatory type of cell death in cardiovascular disease, Clin. Chim. Acta 510 (2020) 62–72, https://doi.org/10.1016/j.cca.2020.06.044.

[13] C. Liu, Q. Yao, T. Hu, Z. Cai, Q. Xie, J. Zhao, et al., Cathepsin B deteriorates diabetic cardiomyopathy induced by streptozotocin via promoting NLRP3-mediated pyroptosis, Mol. Ther. Nucleic Acids 30 (2022) 198–207, https://doi.org/10.1016/j.omtn.2022.09.019.

[14] S. Toldo, E. Mezzaroma, L.F. Buckley, N. Potere, M. Di Nisio, G. Biondi-Zoccai, et al., Targeting the NLRP3 inflammasome in cardiovascular diseases, Pharmacol. Ther. 236 (2022) 108053, https://doi.org/10.1016/j.pharmthera.2021.108053.

[15] A. Wei, J. Liu, D. Li, Y. Lu, L. Yang, Y. Zhuo, et al., Syringaresinol attenuates sepsis-induced cardiac dysfunction by inhibiting inflammation and pyroptosis in mice, Eur. J. Pharmacol. 913 (2021) 174644, https://doi.org/10.1016/j.ejphar.2021.174644.

[16] S. Li, Z. Guo, Z.Y. Zhang, Protective effects of NLRP3 inhibitor MCC950 on sepsis-induced myocardial dysfunction, J. Biol. Regul. Homeost. Agents 35 (1) (2021) 141–150, https://doi.org/10.23812/20-662-a.

[17] S. Gao, H. Chen, Therapeutic potential of apelin and Elabela in cardiovascular disease, Biomed. Pharmacother. 166 (2023) 115268, https://doi.org/10.1016/j.biopha.2023.115268.

[18] A. Mughal, S.T. O'Rourke, Vascular effects of apelin: mechanisms and therapeutic potential, Pharmacol. Ther. 190 (2018) 139–147, https://doi.org/10.1016/j.pharmthera.2018.05.013.

[19] C. Chaves-Almagro, I. Castan-Laurell, C. Dray, C. Knauf, P. Valet, B. Masri, Apelin receptors: from signaling to antidiabetic strategy, Eur. J. Pharmacol. 763 (Pt B) (2015) 149–159, https://doi.org/10.1016/j.ejphar.2015.05.017.

[20] A. Folino, P.G. Montarolo, M. Samaja, R. Rastaldo, Effects of apelin on the cardiovascular system, Heart Fail. Rev. 20 (4) (2015) 505–518, https://doi.org/10.1007/s10741-015-9475-x.

[21] Z. Chen, D. Wu, L. Li, L. Chen, Apelin/APJ system: a novel therapeutic target for myocardial ischemia/reperfusion injury, DNA Cell Biol. 35 (12) (2016) 766–775, https://doi.org/10.1089/dna.2016.3391.

[22] X.J. Zeng, L.K. Zhang, H.X. Wang, L.Q. Lu, L.Q. Ma, C.S. Tang, Apelin protects heart against ischemia/reperfusion injury in rat, Peptides 30 (6) (2009) 1144–1152, https://doi.org/10.1016/j.peptides.2009.02.010.

[23] J. Hu, S. Huo, S. Dou, W. Jiang, Y. Li, Protective effect of Apelin/APJ system on lipopolysaccharide-related cardiac dysfunction, Gen. Physiol. Biophys. 40 (3) (2021) 161–171, https://doi.org/10.4149/gpb_2021006.

[24] X. Liang, Y. Ding, Y. Zhang, Y.H. Chai, J. He, S.M. Chiu, et al., Activation of NRG1-ERBB4 signaling potentiates mesenchymal stem cell-mediated myocardial repairs following myocardial infarction, Cell Death Dis. 6 (5) (2015) e1765, https://doi.org/10.1038/cddis.2015.91.

[25] N. Li, H. Zhou, H. Wu, Q. Wu, M. Duan, W. Deng, et al., STING-IRF3 contributes to lipopolysaccharide-induced cardiac dysfunction, inflammation, apoptosis and pyroptosis by activating NLRP3, Redox Biol. 24 (2019) 101215, https://doi.org/10.1016/j.redox.2019.101215.

[26] W. Gong, H. Wen, Sepsis induced by cecal ligation and puncture, Methods Mol. Biol. 1960 (2019) 249–255, https://doi.org/10.1007/978-1-4939-9167-9_22.

[27] J. Zhang, L. Huang, X. Shi, L. Yang, F. Hua, J. Ma, et al., Metformin protects against myocardial ischemia-reperfusion injury and cell pyroptosis via AMPK/NLRP3 inflammasome pathway, Aging (Albany NY) 12 (23) (2020) 24270–24287, https://doi.org/10.18632/aging.202143.

[28] H. Lin, W. Wang, M. Lee, Q. Meng, H. Ren, Current status of septic cardiomyopathy: basic science and clinical progress, Front. Pharmacol. 11 (2020) 210, https://doi.org/10.3389/fphar.2020.00210.

[29] N. Ravikumar, M.A. Sayed, C.J. Poonsuph, R. Sehgal, M.M. Shirke, A. Harky, Septic cardiomyopathy: from basics to management choices, Curr. Probl. Cardiol. 46 (4) (2021) 100767, https://doi.org/10.1016/j.cpcardiol.2020.100767.

[30] R. Poveda-Jaramillo, Heart dysfunction in sepsis, J. Cardiothorac. Vasc. Anesth. 35 (1) (2021) 298–309, https://doi.org/10.1053/j.jvca.2020.07.026.

[31] J. Zhuang, L. Chen, G. Li, L. Xia, S. Wu, J. Leng, et al., RCAN1 Deficiency Aggravates Sepsis-Induced Cardiac Remodeling and Dysfunction by Accelerating Mitochondrial Pathological Fission, Inflammation research : official journal of the European Histamine Research Society, 2022, https://doi.org/10.1007/s00011-022-01628-5 [et al].

[32] Y.H. Chen, X. Teng, Z.J. Hu, D.Y. Tian, S. Jin, Y.M. Wu, Hydrogen sulfide attenuated sepsis-induced myocardial dysfunction through TLR4 pathway and endoplasmic reticulum stress, Front. Physiol. 12 (2021) 653601, https://doi.org/10.3389/fphys.2021.653601.

[33] Y. Sun, X. Yao, Q.J. Zhang, M. Zhu, Z.P. Liu, B. Ci, et al., Beclin-1-Dependent autophagy protects the heart during sepsis, Circulation 138 (20) (2018) 2247–2262, https://doi.org/10.1161/circulationaha.117.032821.

[34] J.J. Liu, Y. Li, M.S. Yang, R. Chen, C.Q. Cen, SP1-induced ZFAS1 aggravates sepsis-induced cardiac dysfunction via miR-590-3p/NLRP3-mediated autophagy and pyroptosis, Arch. Biochem. Biophys. 695 (2020) 108611, https://doi.org/10.1016/j.abb.2020.108611.

[35] C. Wang, G. Fung, H. Deng, J. Jagdeo, Y. Mohamud, Y.C. Xue, et al., NLRP3 deficiency exacerbates enterovirus infection in mice, Faseb. J. : official publication of the Federation of American Societies for Experimental Biology 33 (1) (2019) 942–952, https://doi.org/10.1096/fj.201800301RRR.

[36] N. Zeng, Z. Jian, J. Xu, S. Zheng, Y. Fan, F. Xiao, DLK1 overexpression improves sepsis-induced cardiac dysfunction and fibrosis in mice through the TGF-β1/Smad3 signaling pathway and MMPs, J. Mol. Histol. 54 (6) (2023) 655–664, https://doi.org/10.1007/s10735-023-10161-6.

[37] D.N. Charo, M. Ho, G. Fajardo, M. Kawana, R.K. Kundu, A.Y. Sheikh, et al., Endogenous regulation of cardiovascular function by apelin-APJ, Am. J. Physiol. Heart Circ. Physiol. 297 (5) (2009) H1904–H1913, https://doi.org/10.1152/ajpheart.00686.2009.

[38] C. Galanth, A. Hus-Citharel, B. Li, C. Llorens-Cortès, Apelin in the control of body fluid homeostasis and cardiovascular functions, Curr. Pharmaceut. Des. 18 (6) (2012) 789–798, https://doi.org/10.2174/138161212799277770.

[39] J. Song, Z. Zhang, Z. Dong, X. Liu, Y. Liu, X. Li, et al., MicroRNA-122-5p aggravates angiotensin II-mediated myocardial fibrosis and dysfunction in hypertensive rats by regulating the elabela/apelin-APJ and ACE2-GDF15-porimin signaling, J Cardiovasc Transl Res 15 (3) (2022) 535–547, https://doi.org/10.1007/s12265-022-10214-3.

[40] K. Kuba, L. Zhang, Y. Imai, S. Arab, M. Chen, Y. Maekawa, et al., Impaired heart contractility in Apelin gene-deficient mice associated with aging and pressure overload, Circ. Res. 101 (4) (2007) e32–e42, https://doi.org/10.1161/circresaha.107.158659.

[41] Y. Peng, R. Jingming, C. Shaowen, H. Feng, Z. Pengli, The protective effect of Apelin-13 against cardiac hypertrophy through activating the PI3K-AKT-mTOR signaling pathway, Iran J Basic Med Sci 26 (2) (2023) 183–189, https://doi.org/10.22038/ijbms.2022.65160.14356.

[42] C.S. Pan, X. Teng, J. Zhang, Y. Cai, J. Zhao, W. Wu, et al., Apelin antagonizes myocardial impairment in sepsis, J. Card. Fail. 16 (7) (2010) 609–617, https://doi.org/10.1016/j.cardfail.2010.02.002.

[43] S. Zhong, H. Guo, H. Wang, D. Xing, T. Lu, J. Yang, et al., Apelin-13 alleviated cardiac fibrosis via inhibiting the PI3K/Akt pathway to attenuate oxidative stress in rats with myocardial infarction-induced heart failure, Biosci. Rep. 40 (4) (2020), https://doi.org/10.1042/bsr20200040.

[44] Y. Liu, J. Shu, T. Liu, J. Xie, T. Li, H. Li, et al., Nicorandil protects against coronary microembolization-induced myocardial injury by suppressing cardiomyocyte pyroptosis via the AMPK/TXNIP/NLRP3 signaling pathway, Eur. J. Pharmacol. 936 (2022) 175365, https://doi.org/10.1016/j.ejphar.2022.175365.

[45] M. Yao, Z. Wang, L. Jiang, L. Wang, Y. Yang, Q. Wang, et al., Oxytocin ameliorates high glucose- and ischemia/reperfusion-induced myocardial injury by suppressing pyroptosis via AMPK signaling pathway, Biomedicine & pharmacotherapy = Biomedecine & pharmacotherapie 153 (2022) 113498, https://doi.org/10.1016/j.biopha.2022.113498.

[46] Y. Ye, Y. Cai, E. Xia, K. Shi, Z. Jin, H. Chen, et al., Apelin-13 reverses bupivacaine-induced cardiotoxicity via the adenosine monophosphate-activated protein Kinase pathway, Anesth. Analg. 133 (4) (2021) 1048–1059, https://doi.org/10.1213/ane.0000000000005692.

[47] J. Tao, W. Zhu, Y. Li, P. Xin, J. Li, M. Liu, et al., Apelin-13 protects the heart against ischemia-reperfusion injury through inhibition of ER-dependent apoptotic pathways in a time-dependent fashion, Am. J. Physiol. Heart Circ. Physiol. 301 (4) (2011) H1471–H1486, https://doi.org/10.1152/ajpheart.00097.2011.
[48] A. Liu, Y. Zhang, S. Xun, G. Zhou, J. Hu, Y. Liu, Targeting of cold-inducible RNA-binding protein alleviates sepsis via alleviating inflammation, apoptosis and oxidative stress in heart, Int. Immunopharm. 122 (2023) 110499, https://doi.org/10.1016/j.intimp.2023.110499.
[49] A. Liu, S. Xun, G. Zhou, Y. Zhang, L. Lin, Honokiol alleviates sepsis-associated cardiac dysfunction via attenuating inflammation, apoptosis and oxidative stress, J. Pharm. Pharmacol. 75 (3) (2023) 397–406, https://doi.org/10.1093/jpp/rgac102.